From Muscle Modeling to Motion: A Full LS-DYNA Workflow with 3D Hybrid Active Muscles in the ANSYS Hans Human Body Model

Mukund Thirugnanasambanthar[1], Michael Ditthardt[2], Christian Kleinbach[2], Oleksandr Martynenko[3], Alexander Gromer[1], Syn Schmitt[3]

[1] Ansys, part of Synopsys
[2] Mercedes-Benz AG
[3] Institut of Modelling and Simulation of Biomechanical Systems (IMSB), University of Stuttgart

1 Introduction

With the onset of higher computing power, detailed Human Body Models (HBMs) are increasingly used in the automotive industry to investigate crashworthiness, occupant protection and pedestrian safety [1]. Passive HBMs have been developed since 2002 [2]. They are employed to analyse kinematics and evaluate injury during in-crash scenarios, but they are limited in their ability to represent muscle activity and reflexive behavior. In contrast, active HBMs (AHBMs) incorporate models of muscles and neuromuscular control, enabling the simulation of physiologically realistic occupant responses accounting for the muscle-driven motion. This capability is particularly important for modelling pre-crash scenarios, where goal-directed movements, reflexes, and voluntary muscle actions significantly influence occupant posture and loading conditions during a crash.

To investigate such behavior, muscle modelling approaches based on Hill-type formulations [5] have been extensively employed due to their computational efficiency and ability to reproduce fundamental force-length and force-velocity relationships. Previous studies have shown that the arm model proposed by Kistemaker [3] combined with the Extended Hill-Type Muscle (EHTM) model [6], provides a suitable framework for exploring control strategies based on the Equilibrium Point Hypothesis (EPH) [7]. This framework allows for the study of muscle activation patterns and neuromuscular control principles underlying goal-directed movements, offering insights into the physiological mechanisms relevant to AHBMs.

However, the one-dimensional formulation of the EHTM restricts the representation of three-dimensional muscle to simple truss elements, which prevents the inclusion of transverse dynamic effects and neglects the complex three-dimensional geometries observed in vivo. To address these limitations, anatomically detailed finite element approaches, such as the Ansys Hans – Human Body Model, have been introduced, offering instruments to capture realistic three-dimensional muscle geometry, mechanics of deformation and material behaviour.

In this study, the authors modified and complemented the arm model proposed by Kistemaker with the EHTM muscles to establish a modelling framework for investigating control strategies in goal-directed muscle-driven motion. The resulting neuro-musculoskeletal model comprises a musculoskeletal model of the arm with one degree of freedom, actuated by four muscles, and a controller. Therefore, it is referred to as Arm14 from here on. Later, we transferred the resulting optimised control strategies to anatomically realistic three-dimensional muscle representations within the Ansys Hans HBM, thereby laying the basis for biofidelic AHBMs.

2 Theoretical background

This section describes a few theoretical concepts related to material models and control theory for goal directed movements.

2.1 1D material models

Active muscle modelling in HBMs has been traditionally carried out using discrete truss elements or beam elements with Hill-type material models. The current material library of LS-DYNA includes some of the 1D muscle material types, such as **`*MAT_SPRING_MUSCLE (*MAT_S15)`** and **`*MAT_MUSCLE (*MAT_156)`** [4]. The 1D representation utilises springs and dampers in various arrangements to mimic the skeletal muscle response, as proposed by Hill [5]. The **`*MAT_S15`** represents the Hill-type model, which uses a Contractile element (CE) connected in series with a Serial

Elastic Element (SEE) and a Parallel Elastic Element (PEE) in parallel. The total force of the muscle is computed as the sum of CE and PEE forces. The ***MAT_MUSCLE** is an extension of the ***MAT_S15** with a parallel damping element added for increased stability and to reduce high-frequency oscillations during contractions. While these models are widely used, they are both based on empirical relations that are neither muscle specific nor derived from anatomical textbooks. Inputs in the material cards, such as relative length, shortening velocity and dimensionless parameters, including tensile stress as a function of stretch ratio and strain rate, require curves that are difficult to obtain from the literature and demand tuning using optimization methods to fit specific objectives.
As an example, the contractile element force F_{CE} for ***MAT_S15** is given as:

$$F_{CE} = a\,(t) * F_{max} * f_{TL}(L) * f_{TV}(V)$$

where $a\,(t)$ – the load curve for muscle activation, F_{max} – maximum isometric force of the muscle, $f_{TL}(L)$ - tension-length relation and $f_{TV}(V)$- tension-velocity relationship. Except for the F_{max} other parameters are not specific to the modelled muscle and need to be optimized through curve fitting.

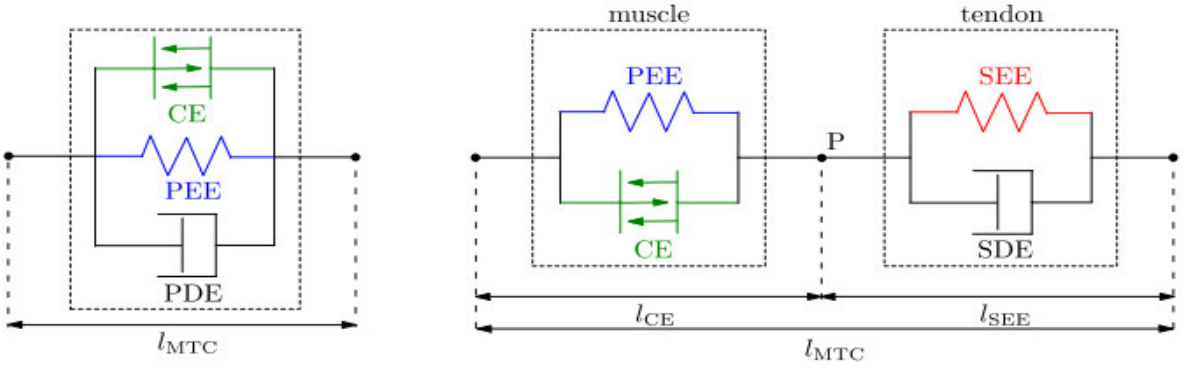

*Fig.1: Schematic representation of *MAT_156 and EHTM internal structures [6]*

The EHTM model is an open-source material model that mimics complete muscle tendon unit (MTU). Unlike the ***MAT_MUSCLE** and ***MAT_S15** models, the EHTM utilizes muscle specific data, such as maximum isometric force, muscle length, along with non-specific parameters or constants that are available in the literature. The conventional force in the EHTM is based on the equilibrium between the muscle and tendon unit and is modelled as follows:

$$Force_{Muscle} = Force_{Tendon}$$

$$F_{CE}(l_{CE}, \dot{l}_{CE}, q) + F_{PEE}(l_{CE}) = F_{SEE}(l_{MTU}, l_{CE}) + F_{SDE}(l_{CE}, \dot{l}_{CE}, \dot{l}_{MTU}, q)$$

where l_{CE} – length of the muscle, l_{SEE}-length of tendon, l_{MTU} – length of MTU= l_{CE} + l_{SEE}, $\dot{l}_{CE}$ – contraction velocity of CE, q – muscle activity. The material model also computes muscle activation level internally during runtime based on stimulation values from a controller through various integrated activation dynamics, such as Hatze, modified Hatze and Zajac. The EHTM comes with a PID controller featuring 4 strategies: an open-loop, a closed-loop length feedback, a hybrid controller and a reflex-based controller [8]. The control loops are placed within the Fortran material subroutine and are executed faster than standard LS-DYNA Keyword read statements [8]. These conditions make EHTM a suitable candidate for use in the development of AHBMs.

2.2 3D continuum-based models

3D material models offer a more biofidelic solution to finite element modelling problems such as routing, that arise from the use of 1D beams to model active muscles. Previous studies on developing 3D material models have worked with the assumption to model the muscle as a transversely isotropic hyperelastic model [9, 10, 11, 12] or viscoelastic model with dispersed fibres [13]. However, in most previous studies, the modelling method is limited specific part of the body, such as the antagonistic muscle group in the upper arm [9,10,11] or the upper leg [14] or a single muscle test [13]. Due to the computational complexity and the lack of an effective muscle control strategy, scaling full HBM remains a challenge. From the library of LS-DYNA, there exist ***MAT_TISSUE_DISPERSED** and ***MAT_ANISOTROPIC_HYPELASTIC**. These are material models used to model cardiac muscles. With a slight modification to material parameters, they can be used to represent skeletal muscles [15]. The

activation part of these models requires an electromagnetic solver, which limits their use in typical HBM use cases.

2.3 Hybrid muscle model

Hybrid muscle modelling is not directly a material model, but rather a combination of 2 different models connected by common nodes. Active 1D Hill-type models are coupled with a passive muscle structure. The concept has been explored in the past by Hedenstierna et al. [16], who combined 1D truss elements with 3D viscoelastic and hyperelastic models. A similar technique was also attempted by combining **`*MAT_MUSCLE`** and **`*MAT_181`** to implement a hybrid model [17][18][19].

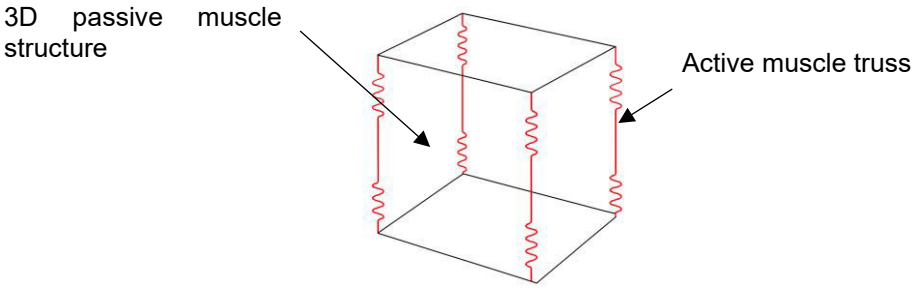

Fig.2: Schematic representation of a hybrid modelling technique

An additive decomposition of the Cauchy stresses between the active and the passive parts sets the basis for this type of modelling.

$$\sigma_{total} = \sigma_{passive} + \sigma_{active}$$

Where the σ_{active}- $F_{active}/PCSA$, $PCSA$ – refers to the physiological cross-section of the muscle, an information available in literature. F_{active} – can have different formulations based on the choice of material model. $\sigma_{passive}$- is the stress from the 3D passive model. The hybrid modelling also keeps the whole development of AHBMs modular. This is an advantage as most HBMs are already validated for the passive response and have tuned material parameters to match test corridors for high velocity events.

2.4 Equilibrium-Point Hypothesis

Rapid, goal-directed single-joint movements represent a classic challenge for motor control theories, particularly due to the high demands on temporal precision and dynamic stability. Kistemaker et al. [3] investigated in an influential study whether such movements can also be realized through so-called Equilibrium-Point Hypothesis (EPH) of motor control. This control concept assumes movements arise from a shift in a virtual equilibrium point, rather than through explicit calculation of torques or trajectories (inverse dynamics).

The EPH was initially proposed by [20] and further developed in later works [21]. It assumes that the central nervous system controls movements through the gradual adjustment of muscular activation thresholds – without explicitly specifying forces or end positions. Numerous studies have shown that this theory is well-suited to explain slow or reflex-mediated movements. However, it remained controversial whether it is also practicable for fast, targeted movements [22].

To verify this question, in [3] a biomechanically realistic musculoskeletal model of the human arm (elbow) was used, which maps musculoskeletal properties such as force-length-velocity relationships, viscoelastic tendon elements, and reflex behavior. Within this model, multiple control approaches were investigated, including the open-loop α-controller. This controller refers to the relationship between α-motoneuron activation and the associated equilibrium point (EP).

3 Arm14 model within Ansys Hans

To simulate muscle-driven movements in HBM, it is necessary not only to implement active muscles but also to install a control strategy to govern them. EPH is utilized in this study to control muscle-driven movements in the HBM Ansys Hans arm. Theory states that a particular body posture corresponds to a specific equilibrium point of the muscles.

To validate the simulation approach, the experiment from [3] was replicated with an Arm14 model. The authors performed muscle-driven control of various arm positions extracted from the HBM. The simulation results serve to evaluate the applicability of the EPH for movement control within the whole Ansys Hans model.

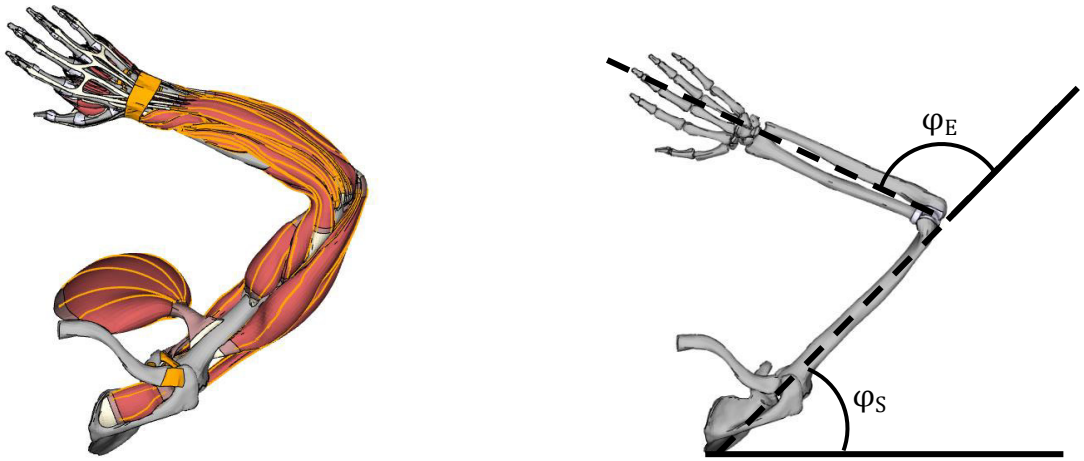

Fig.3: Experimental setup of the Arm14 model with shoulder and elbow angle definitions [3]

3.1 Modelling Set-up

For the analysis and determination of the various EPs, a reduced arm model of the HBM Ansys Hans was utilized (Fig. 4). In the first step, the arm is positioned in the transversal plane, analogous to the experiment conducted in [3]. To determine muscle routing, moment arms, and muscle stimulation values (STIM), a multi-body model with rigid bone structures was initially constructed, where bones are represented as rigid bodies. The rotational connection between the forearm (ulna and radius) and the upper arm (humerus) is modeled by a revolute joint, implemented via the **`*CONSTRAINED_JOINT_REVOLUTE`** definition in LS-DYNA. The humerus and shoulder are fixed in the global coordinate system with the material card **`*MAT_RIGID`** in all degrees of freedom, allowing only muscle-driven rotation of the forearm about the joint axis.

Mass contributions from three-dimensional muscles, skin, and other soft tissues, which were removed in the second step of model reduction, are represented by **`*ELEMENT_MASS`** distributed on the nodes of the forearm and upper arm. This approach ensures that the total mass and inertia properties of the reduced arm model correspond to those of the original Ansys Hans arm.Muscles are modeled using extended Hill-type muscle models (EHTM) [6] with **`*MAT_USER_DEFINED_MATERIAL_MODELS`** and are represented in the simulation as one-dimensional beam elements. Following the methodology suggested in [3], muscles are not modeled individually but are grouped into four functional muscle groups with the corresponding muscle properties:

- Monarticular Elbow Flexor (MEF)
- Monarticular Elbow Extensor (MEE)
- Biarticular Elbow Flexor with Shoulder Anteversion (BEFSA)
- Biarticular Elbow Extensor with Shoulder Retroversion (BEESR)

Fig.4: From the full Ansys Hans arm to the reduced optimization Arm14 model

The origin and insertion points of the muscle groups are based on a predecessor project and roughly correspond to the attachment points reported by [3]. The initial routing points around the joint of each muscle group were manually defined in the transversal plane and subsequently optimized based on moment arm trajectories.

For the initial simulations, the LS-DYNA material cards for muscle-specific parameters are based on the studies by Kistemaker et al. [3] and Wochner et al. [23]. The non-specific muscle parameters required are taken from the works of van Soest and Bobbert [24], Mörl et al. [25], and Kleinbach et al. [6]. This approach enables a well-founded and detailed parametrization of the models, incorporating both individual muscle physiological properties and general biomechanical characteristics.

3.2 Optimization of the Arm14 model

Muscle moment arms at the elbow joint play a central role in generating movement and determining the full range of motion (ROM). The moment arm represents the effective lever length by which the axial tensile force generated by the muscle is converted into a moment around the joint. Formally, the moment arm ma is defined as the shortest distance between the muscle's line of action and the joint axis [26] (Fig. 5).

In simplified muscle-driven multi-body models, the muscle is often represented as a straight line connecting its origin and insertion points. This is illustrated by the brachialis muscle (BRA) in Fig. 5, where D_l represents the long distance and D_s the short distance between the joint and the muscle origin/insertion point and ma the moment arm of the muscle. While this assumption simplifies the calculation, it does not account for the anatomically realistic muscle paths. In the human body, muscles do not run straight but rather wrap around bones, joints, and soft tissue structures, which is especially relevant for complex joints such as the elbow. A specific problem arises primarily in the modeling of the extensors: when these muscle paths intersect the joint axis, the model can exhibit an unphysiological switch in moment arms, causing the extensors to act as flexors incorrectly. To address this issue, so-called routing points are integrated into the model, representing the muscle path along anatomically realistic trajectories. The moment arm is calculated separately for each muscle segment between two routing points, resulting in a more accurate representation of the muscle moment arm.

This approach enables improved simulation of the full range of motion and prevents erroneous movement representations by anatomically correctly accounting for the direction and length of the moment arms.

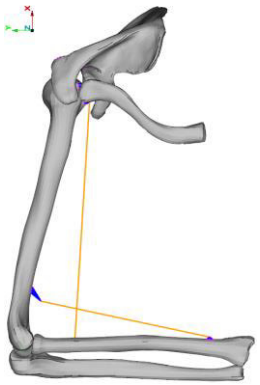

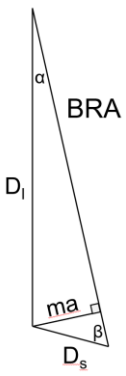

Fig.5: A simple implementation of 1D muscles in the Ansys Hans Arm14 model and the definition of the moment arm ma based on literature [25]

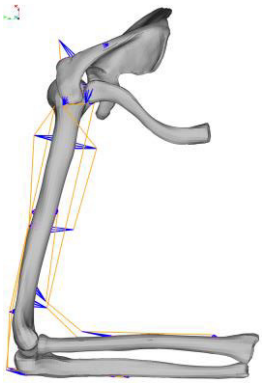

Fig.6: Muscle routing paths with specific routing points of the lumped muscles in the Ansys Hans Arm14 model

As described in the previous section, the initial definition of routing points is performed in the transverse plane based on the moment arm trajectories of the human arm. To increase anatomical accuracy and ensure a full range of motion, the routing point positions are optimized. For this purpose, Metamodel-Based Optimization (MBO) using the Sequential Response Surface Method (SRSM) as the optimization strategy is employed in the software LS-OPT.

In this approach, the coordinates of the routing points are modeled as decision variables and approximated using polynomial surrogate models, specifically, linear functions. The selection of sample points is performed using a D-optimal design strategy, which maximizes the information content of the samples [27]. The objective of the optimization is to maximize the range of motion while considering predefined muscle parameters, to represent best the moment arm profile of individual muscle groups over the entire joint angle range.

Validation and comparison of the optimized moment arm trajectories are carried out based on the work by Wochner [23] and Suissa [28]. These reference data serve as benchmarks to ensure the physiological plausibility and accuracy of the modeled muscle moment arms.

To ensure a full range of motion for both elbow flexion and extension, the initial muscle parameters in the material cards must be adjusted. These adjustments are based on the force-length and force-velocity relationships of muscles, as well as the EHTM muscle-specific parameters. Specifically, both the length of the contractile element l_{CE} and the tendon slack length $l_{SEE,0}$ was modified to enable complete flexion and extension movements (Fig. 7). In combination with the adjusted moment arms, such calibration ensures that the muscle stimulation values STIM for the individual equilibrium points can be accurately determined in subsequent analyses.

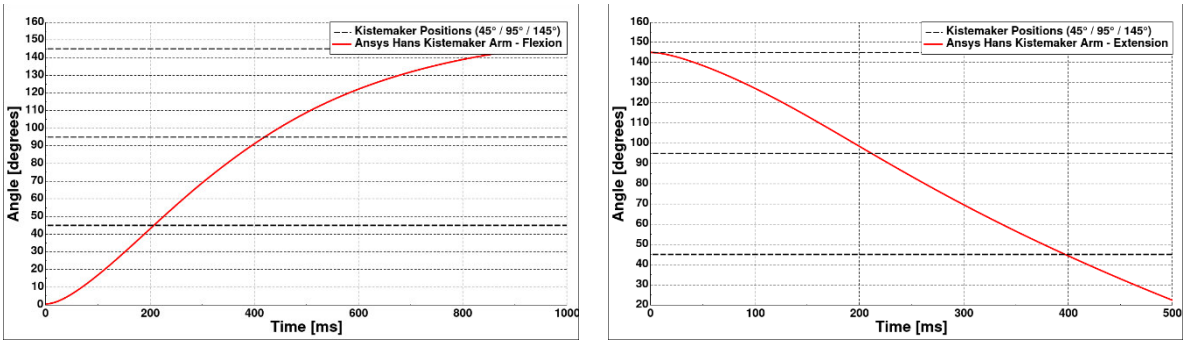

Fig.7: Full Range of Motion (ROM) Simulations for flexion (left) and extension (right)

3.3 Optimization of the controller

Based on the EPH, each elbow joint angle corresponds to a specific equilibrium state EP, achieved through a defined activation pattern of the muscles involved. Consequently, the optimization of stimulation parameters (STIM values) for the four muscle groups is performed separately for each target angle. The resulting STIM values can then be sequentially applied in a time-dependent simulation to generate continuous, muscle-driven arm movements.

To replicate the experiment from Kistemaker et al. [3], three target positions are defined, each differing by 50° in the elbow angle. The shoulder angle φ_S, defined as the angle between the upper arm and the coronal plane (see Fig. 3), is fixed at 45° throughout the entire experiment. The elbow angle φ_E is set to three distinct values: 45°, 95°, and 145°, corresponding to positions 1-3 of the experiment.

The LS-OPT optimization follows the same structural setup as the routing point optimization described in Section 3.2. However, instead of nodal coordinates, the STIM values were optimized, which govern muscle activation and are stored in the material card. In addition to reaching the target joint angle (EP) it is essential to guarantee that the angular velocity at the final time step is approximately zero. A stable equilibrium state, as defined by the EP, can only be assumed under these conditions.

3.4 Validation of model and controller

Following the determination of STIM values for individual positions within the optimization processes, muscle-driven movements are simulated using these STIM values. Arm flexion occurs stepwise from position 1 – 45° over position 2 – 95° to position 3 – 145°, followed by arm extension in one motion from position 3 back to position 1. Each position must be held for a specific duration to allow the development of EP.

As shown in Fig. 8, the initial angle of 45° is maintained exclusively by the open-loop α-controller. During the transition to the second position (95°), a slight deflection is initially observed. This is attributed to the

adjustment of EPs within the EHTM muscle elements, particularly in the interaction between contractile elements (CE) and tendon (SEE). The movement to the second position is realized within approximately 2000 ms. However, a stable EP does not establish here, as minimal rotation at the elbow joint continues to be observed until the transition to the third position. The transition from position 2 to position 3 (145°) occurs more quickly, and the corresponding EP stabilizes again. For the subsequent arm extension, the muscles are activated in such a way that the starting position is directly targeted. A stable EP does not form here either and a continuous rotation is apparent.

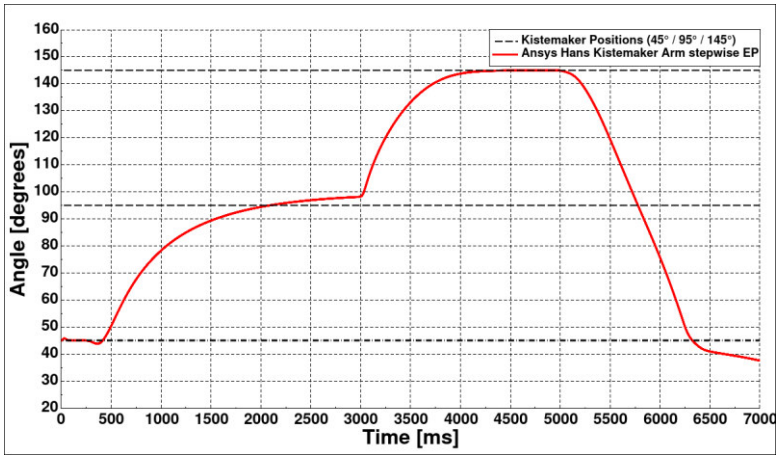

Fig.8: Validation of specific Equilibrium-Points with Ansys Hans Kistemaker Arm

Investigations of various STIM patterns for the middle and end positions showed that the EPs cannot be set precisely. This limitation results from the combination of the lever arms of the muscles around the elbow joint with the optimized muscle parameters, which are stored in the material cards. Since the model represents muscle groups, experimental validation of the muscle parameters is not possible. For this reason, the modeling is based on established works [3,23] and adjusts the muscle parameters in a way that allows for realistic movements to be achieved. For better improvement, optimization loops would be required to adjust both lever arms and muscle parameters simultaneously. However, the adjustment of muscle parameters is done using an external Python script and is not coupled with the LS-OPT optimization tool. This is currently a limitation, and such a coupled optimization is considered as future work.

The implementation of muscles using one-dimensional beam elements within the EHTM muscle material model represents a simplified representation of active muscles in HBMs, without any link between the longitudinal and the transversal direction of the muscles. Furthermore, the definition of routing points and muscle moment arms represents a simplification of the model, as the realistic routing of the musculature based on its three-dimensional geometry cannot be represented.

4 Validating a hybrid muscle modelling approach

The EHTM with its in built muscle control strategies shows a good potential to develop a HBM that can perform goal directed movements using one dimensional beam elements. For subsequent use in the study, it is also necessary to check the feasibility of utilising it for three-dimensional hybrid muscle modelling. To validate the hybrid modelling approach, an individual muscle was tested at the system level for its contraction properties and the fundamental force-length relationship, which is central to modelling active muscles.

4.1 Stress-strain relation

Experimental data from Myers et al. [29] was used to validate the modelling method. A rabbit's tibialis anterior (TA) muscle was elongated with three different strain rates: 1, 10 and 25 Hz. The muscle was 90 mm long with a mid-muscle belly cross-sectional area of 45 mm^2. One end of the muscle was fixed with the keyword **`*BOUNDARY_SPC`** in all degrees of freedom. In contrast, the other end had a **`*BOUNDARY_PRESCRIBED_MOTION`** applied to stretch the muscle in the global X-direction (Fig. 9). While the 3D passive muscle structure is modelled using **`*MAT_181`**, the active part is tested with two different material models: **`*MAT_S15`** and default EHTM. The **`*MAT_S15`** was used instead of **`*MAT_MUSCLE`** as their properties are similar, and the simulation can be executed with minimal tuning for material parameters. The muscle activation was based on Hatze activation dynamics. The prescribed motion is applied after the muscle has been completely activated. The termination time is computed as

the time taken to have 25% of strain. A cross-section is defined at the middle of the muscle belly to measure the stress.

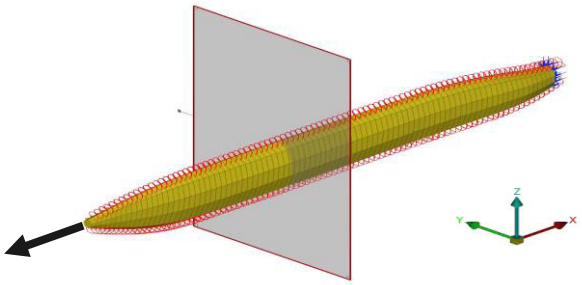

Fig.9: Boundary condition for the stress strain-validation simulation

4.2 Force-length relationship

The test for the isometric force-length relationship is based on the test prescribed in Iwamoto et al. (2009) [17]. A simplified muscle model is given a constant activation value of 0.3, fixed at one end and extended at the other end using a normalised velocity curve as given in Fig. 10. While this simulation is a method for fitting the force-length relationship curve that needs to be input into the material card for **`*MAT_S15`**, this analysis can demonstrate how well the EHTM can predict corresponding forces.

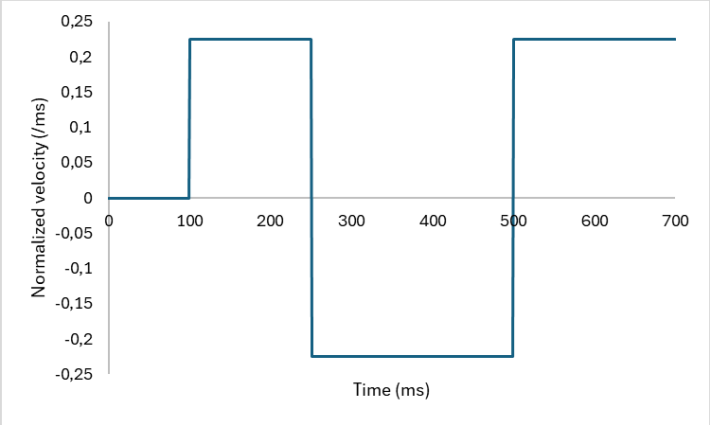

Fig.10: Normalized velocity applied to the free end.

4.3 Results

4.3.1 Stress-strain response

The stress developed in the muscle belly was also evaluated against the other material models and earlier studies. Table 1 shows the comparison of the normalised root mean square error of the different models with the experimental data. During simulation runs, it was learnt that the default EHTM had a very stiff response and had a bad stress-strain correlation, therefore a modified EHTM was introduced and tested too. The modified EHTM is an extraction from the complete model, which executed only the muscle part of the material model. The corresponding changes were made in the user material subroutine.

Table1. Simulation setup vs NRMSE

Simulation setup	NRMSE
Khodaei et al. [13]	33%
Hedenstierna et al. [16]	20%
Fernandes et al. [15]	17%
Mat_S15	17%
Default EHTM	42%
Modified EHTM	15%

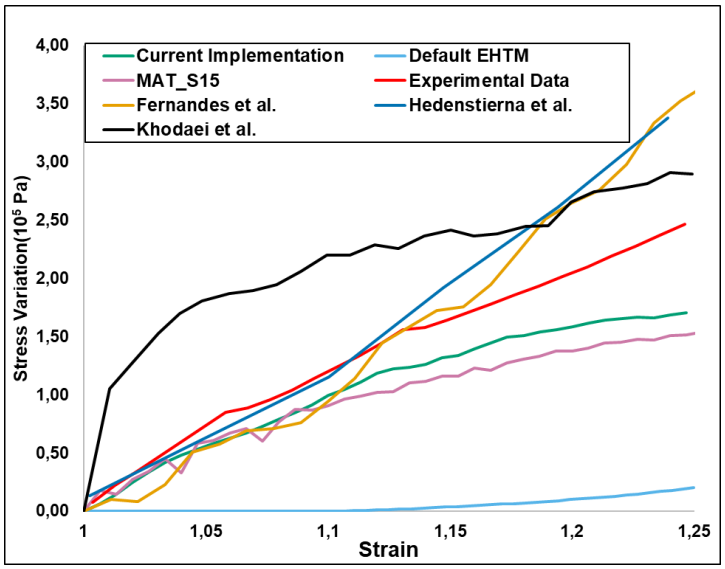

Fig.11: Stress variation for different material models used in hybrid setting

As seen from the results, the implementations of Fernandes et al. [15], **`*MAT_S15`** and modified EHTM show the lowest deviation from the experiment. The limitations, though, are evident in the first 2 models: Fernandes et al. [15] used **`*MAT_TISSUE_DISPERSED`** which is obsolete, and while **`*MAT_S15`** exhibits a good stress-strain comparison, there is necking and uneven extension at high strains (Fig. 13). The modified EHTM is much more stable and has the lowest error, making it a good candidate for use in hybrid muscle modelling.

A) B)

Fig.12: Final time step: A) modified EHTM, B) **`*MAT_S15`**

4.3.2 Force-length relationships

The validation of the muscle isometric force-length relationships was performed only for the modified EHTM with the passive **`*MAT_181`** material model. The normalised force-length relationship as seen in Fig. 14 is consistent with the model used by Iwamoto et al. (2009) [17][30]. As seen the model is still not able to reach higher strains, but this can be achieved by parameters variation in the material input card.

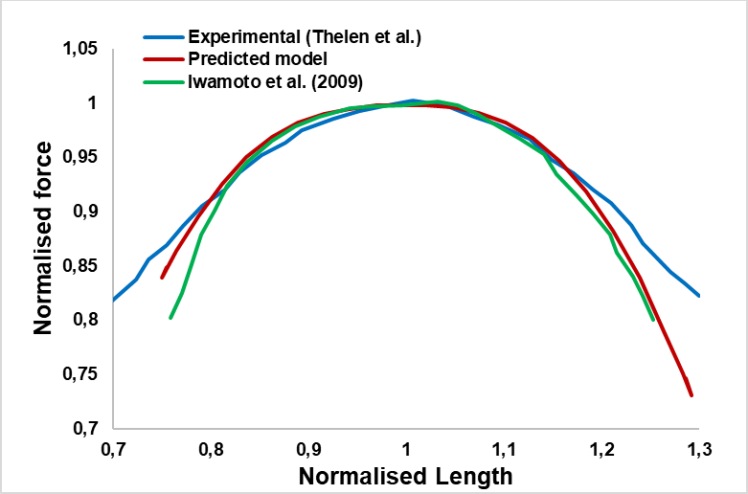

Fig.13: Force-length relationship

5 Summary and Outlook

Current state-of-the-art HBMs exhibit notable limitations in accurately representing neuromuscular dynamics. To address these shortcomings, a simplified Arm14 model was developed based on the ANSYS Hans HBM and validated against experimental data [3]. The model employed rigid bones and one-dimensional muscles, with integrated motor control strategies implemented using the EPH. This framework allowed the testing and refinement of control strategies prior to extending them to more complex models with deformable bones and anatomically detailed musculature. Although this approach enabled the extraction of valuable information, such as stimulation and activation patterns for specific upper-limb configurations, it required extensive optimization and proved to be repetitive and computationally demanding.

To overcome these challenges, a hybrid modelling approach is proposed as a more efficient and physiologically representative alternative. Initial tests at the muscle-tendon unit level demonstrated the ability of this method to reproduce contraction dynamics with high fidelity. However, several limitations remain. For example, the effects of impact loading on activated muscles have not yet been systematically investigated, and physiological factors, such as pennation angle, must be integrated to ensure accurate representation of resultant muscle forces within the active structure.

Future work will focus on implementing stimulation patterns obtained from optimization studies into the ANSYS Hans arm model using the hybrid approach. This step enables the transition from simplified representations to models that can capture complex musculoskeletal interactions. Based on the initial outcomes, further research may be required to develop advanced control strategies, including higher-level controllers that regulate joint angles, spatial tuning, and coordinated muscle activation. Such developments would significantly enhance the predictive capability and applicability of HBMs in biomechanical research and impact analysis.

6 Acknowledgement

This technical conference paper was written as part of the ‘CARpulse’ Project, funded under the code 02P23Q800 by the Federal Ministry of Education and Research (BMBF) by decision of the German Bundestag and supervised by the Project Management Agency Karlsruhe (PTKA). The authors would like to thank Tobias Erhart for sharing his valuable knowledge in LS-DYNA User Interfaces and helpful advice. The consortium partners would like to thank BMBF and the PTKA for its support. The responsibility for the content lies with the authors.

7 Literature

[1] Mokhtar, A. A., & Hyncik, L. (2024). *A comprehensive review of human body model in different crash scenarios: Active and passive models*. *International Journal of Crashworthiness, 30*(1), 1-13. https://doi.org/10.1080/13588265.2024.2352242

[2] Iwamoto, M., Kisanuki, Y., Watanabe, I., Furusu, K., Miki, K., & Hasegawa, J. (2002, September). *Development of a finite element model of the Total Human Model for Safety (THUMS) and application to injury reconstruction*. In *Proceedings of the 2002 International IRCOBI Conference on the Biomechanics of Impact* (pp. 31-42). Munich, Germany.

[3] Kistemaker, D. A., et al.: “Is Equilibrium Point Control Feasible for Fast Goal-Directed Single-Joint Movements?”, Journal of Neurophysiology, Vol. 95, pp. 2898–2912, 2006.

[4] *ANSYS LS-DYNA® Keyword User's Manual Volume II: Material Models* (R16). Retrieved from https://lsdyna.ansys.com/wp-content/uploads/2025/04/LS-DYNA_Manual_Vol_II_R16.pdf

[5] Hill, A. V. (1938). The heat of shortening and the dynamic constants of muscle. Proceedings of the Royal Society of London. Series B, 126, 136–195.

[6] Kleinbach, C., et al.: „Implementation and validation of the extended Hill-type muscle model with robust routing capabilities in LS-DYNA for active human body models”, Biomedical engineering online 16.1, 109, 2017

[7] Martynenko, O. V., Kempter, F., Kleinbach, C., et al. (2023). Development and verification of a physiologically motivated internal controller for the open-source extended Hill-type muscle model in LS-DYNA. *Biomechanics and Modeling in Mechanobiology, 22*, 2003–2032. https://doi.org/10.1007/s10237-023-01748-9

[8] Wochner, I., Endler, C. A., Schmitt, S., et al. (2019). Comparison of controller strategies for active human body models at the example of different muscle materials. In *Proceedings of the*

International IRCOBI Conference (pp. 133–134). IRCOBI Council. http://www.ircobi.org/wordpress/downloads/irc19/pdf-files/30.pdf

[9] Sprenger, M. (2015). *A 3D continuum-mechanical model for forward-dynamics simulations of the upper limb* (PhD thesis). University of Stuttgart, Institute for Mechanics, Chair of Continuum Mechanics.

[10] Röhrle, O., Sprenger, M., & Schmitt, S. (2017). A two-muscle, continuum-mechanical forward simulation of the upper limb. *Biomechanics and Modeling in Mechanobiology, 16*(4), 743–762. https://doi.org/10.1007/s10237-016-0850-x

[11] Saini, H., & Röhrle, O. (2022). A biophysically guided constitutive law of the musculotendon-complex: Modelling and numerical implementation in Abaqus. *Computer Methods and Programs in Biomedicine, 226*, 107152. https://doi.org/10.1016/j.cmpb.2022.107152

[12] Avci, O., & Röhrle, O. (2024). Determining a musculoskeletal system's pre-stretched state using continuum–mechanical forward modelling and joint range optimization. *Biomechanics and Modeling in Mechanobiology, 23*, 1031–1053. https://doi.org/10.1007/s10237-024-01821-x

[13] Khodaei, H., Mostofizadeh, S., Brolin, K., Johansson, H., & Östh, J. (2013). Simulation of active skeletal muscle tissue with a transversely isotropic viscohyperelastic continuum material model. *Proceedings of the Institution of Mechanical Engineers, Part H: Journal of Engineering in Medicine*, *227*(5), 571-580.

[14] Li, J., Lyu, Y., Miller, S., Jin, Z., & Hua, X. (2019). Development of a finite element musculoskeletal model with the ability to predict contractions of three-dimensional muscles. *Journal of Biomechanics, 94*, 109341. https://doi.org/10.1016/j.jbiomech.2019.07.042

[15] Fernandes, N. A. T. C., Schmitt, S., & Martynenko, O. V. (2019, July). Modelling and validation of the 3D muscle-tendon unit with solid finite elements in LS-DYNA for active human body model applications. In *Conference proceedings of the International Research Council on the Biomechanics of Injury (IRCOBI), Florence, Italy.*

[16] Hedenstierna, S., Halldin, P., & Brolin, K. (2008). Evaluation of a combination of continuum and truss finite elements in a model of passive and active muscle tissue. *Computer methods in biomechanics and biomedical engineering*, *11*(6), 627–639. https://doi.org/10.1080/17474230802312516

[17] Iwamoto, M., Nakahira, Y., Kimpara, H., & Sugiyama, T. (2009). Development of a human FE model with 3-D geometry of muscles and lateral impact analysis for the arm with muscle activity. *SAE Technical Papers.* https://doi.org/10.4271/2009-01-2266

[18] Putra, I. P. A., Carmai, J., Koetniyom, S., & Markert, B. (2015, June). The effect of active muscle contraction on pedestrian kinematics and injury during vehicle–pedestrian collision. In *10th European LS-DYNA Conference 2015, Würzburg, Germany.*

[19] Mo, F., Li, F., Behr, M., et al. (2018). A lower limb–pelvis finite element model with 3D active muscles. *Annals of Biomedical Engineering, 46*(1), 86–96. https://doi.org/10.1007/s10439-017-1942-1

[20] Feldman, A. G.: "Functional tuning of the nervous system with control of movement or maintenance of a steady posture – II. Controllable parameters of the muscle." Biophysics, Vol. 11, pp. 565–578, 1966.

[21] Latesh, M. L., et al.: "Motor Control Theories and Their Applications", Medicina (Kaunas), 46(6), pp. 382–392, 2010.

[22] Gribble, P. L., et al.: "Are Complex Control Signals Required for Human Arm Movement?", Journal of neurophysiology 79.3, pp. 1409-1424, 1998

[23] Wochner, I.: "The benefit of muscle-actuated systems: internal mechanics, optimization and learning", Institute for Modelling and Simulation Biomechanical Systems, University of Stuttgart, 2023

[24] van Soest, A. J., Bobbert, M. F.: "The contribution of muscle properties in the control of explosive movements", Biological cybernetics, 69(3): 195-204, 1993

[25] Mörl, F., et al.: "Electro-Mechanical Delay in Hill-Type Muscle Models.", Journal of Mechanics in Medicine and Biology, 12.05, 1250085, 2012

[26] Murray, W. M., et al.: "Scaling of peak moment arms of elbow muscles with upper extremity bone dimensions", Journal of Biomechanics 35, pp. 19-26, 2002

[27] Kleijnen, J.P.C.: "Regression and Kriging Metamodels with Their Experimental Designs in Simulation: Review.", CentER Discussion Paper, vol. 2015-035, CentER, Center for Economic Research, Tilburg, 2015.

[28] Suissa, D.R.: "Modeling, Control and Optimization in Human Motor Control: A Simulation Study of a Physiological Human Arm", Institute for Modelling and Simulation Biomechanical Systems, University of Stuttgart, 2017

[29] Myers, B. S., Woolley, C. T., Slotter, T. L., Garrett, W. E., & Best, T. M. (1998). The influence of strain rate on the passive and stimulated engineering stress--large strain behavior of the rabbit tibialis anterior muscle. *Journal of biomechanical engineering*, *120*(1), 126–132. https://doi.org/10.1115/1.2834292

[30] Thelen D. G. (2003). Adjustment of muscle mechanics model parameters to simulate dynamic contractions in older adults. *Journal of biomechanical engineering*, *125*(1), 70–77. https://doi.org/10.1115/1.1531112